

Dark Matter Detectors as Dark Photon Helioscopes

Haipeng An,¹ Maxim Pospelov,^{1,2} and Josef Pradler³

¹*Perimeter Institute, Waterloo, Ontario N2L 2Y5, Canada*

²*Department of Physics and Astronomy, University of Victoria, Victoria, BC, V8P 5C2, Canada*

³*Department of Physics and Astronomy, Johns Hopkins University, Baltimore, MD 21210, USA*

Light new particles with masses below 10 keV, often considered as a plausible extension of the Standard Model, will be emitted from the solar interior, and can be detected on the Earth with a variety of experimental tools. Here we analyze the new “dark” vector state V , a massive vector boson mixed with the photon via an angle κ , that in the limit of the small mass m_V has its emission spectrum strongly peaked at low energies. Thus, we utilize the constraints on the atomic ionization rate imposed by the results of the XENON10 experiment to set the limit on the parameters of this model: $\kappa \times m_V < 3 \times 10^{-12}$ eV. This makes low-threshold Dark Matter experiments the most sensitive dark vector helioscopes, as our result not only improves current experimental bounds from other searches by several orders of magnitude, but also surpasses even the most stringent astrophysical and cosmological limits in a seven-decade-wide interval of m_V . We generalize this approach to other light exotic particles, and set the most stringent direct constraints on “mini-charged” particles.

Introduction The Standard Model (SM) of particle physics based on the gauge group structure $G_{SM} = \text{SU}(3)_c \times \text{SU}(2)_L \times \text{U}(1)_Y$ and the Higgs mechanism is now firmly established and confirmed in a wide range of energies. At the same time there are reasons to think that SM is an effective theory, and new ingredients must be added to it. New states may exist both at higher energy scales with sizable couplings to SM, and at low energies where such states would have to be neutral under G_{SM} and very weakly coupled to the SM particles. Among the few distinct classes to couple new light states to the SM singlet operators, the $\text{U}(1)_Y$ hypercharge field strength appears as the most natural [1]. It is singled out not only by its minimality but by its enhancement in the infrared (IR). The hypercharge portal leads to the mixing of an additional $\text{U}(1)_V$ gauge boson (called “dark photon” from here on) with the SM photon, and thus can easily manifest itself in low-energy phenomena.

In the last few years, the model of kinetically mixed vectors has received tremendous attention, theoretically as well as experimentally. While the mass range above ~ 1 MeV is mostly subjected to traditional particle physics constraints with high-intensity beams, the intermediate mass range, 10 eV to 1 MeV, is much constrained by astrophysics and cosmology. In the lowest mass range, $m_V < 10$ eV, astrophysical limits are complemented by direct laboratory searches of dark photons in non-accelerator type experiments. A collection of low-energy constraints on dark photons can be found in the recent review [2]. Among the most notable detection strategies are the “light-shining-through-wall” experiments (LSW) [3] and the conversion experiments from the solar dark photon flux, “helioscopes” [4]. The latter class of experiments derives its sensitivity from the fact that such light vectors are readily excited in astrophysical environments, such as *e.g.* in the solar interior, covering a wide range of masses up to $m_V \sim \text{few keV}$. Stellar astrophysics pro-

vides stringent constraints on any type of light, weakly-interacting particles when the emission becomes kinematically possible [5]. Only in a handful of examples does the sensitivity of terrestrial experiments match the stellar energy loss constraints.

In a recent work [6] we have identified a new stellar energy loss mechanism originating from the resonant production of longitudinally polarized dark photons. Ref. [6] significantly improved limits on dark photons compared to the original analysis [4], to the extent that all current LSW and helioscope experiments now find themselves deep inside astrophysically excluded regions.

The purpose of this letter is to show that the newly calculated flux of dark photons in combination with utmost sensitivity of direct Dark Matter detection experiments to atomic ionization make a powerful probe of dark photon models. In what follows, we calculate the solar flux of dark photons, both for the case of a “hard” Stueckelberg mass m_V and for a mass originating from Higgsing the $\text{U}(1)_V$. After that we compute the atomic ionization rates from dark photons, taking full account of the medium effects, to derive powerful constraints on the parameter space of the model using the results of the XENON10 experiment.

Dark Photons The minimal extension of the SM gauge group by an additional $\text{U}(1)_V$ gauge factor yields the following effective Lagrangian well below the electroweak scale,

$$\mathcal{L} = -\frac{1}{4}F_{\mu\nu}^2 - \frac{1}{4}V_{\mu\nu}^2 - \frac{\kappa}{2}F_{\mu\nu}V^{\mu\nu} + \frac{m_V^2}{2}V_\mu V^\mu + eJ_{\text{em}}^\mu A_\mu, \quad (1)$$

where V_μ is the vector field associated with the Abelian factor $\text{U}(1)_V$. The field strengths of the photon $F_{\mu\nu}$ and of the dark photon $V_{\mu\nu}$ are connected via the kinetic mixing parameter κ where a dependence on the weak mixing angle was absorbed; J_{em}^μ is the usual electromagnetic current with electric charge e .

Because of the $U(1)$ nature of (1), we must distinguish two cases for the origin of m_V : the Stueckelberg case (SC) with non-dynamical mass, and the Higgs case (HC), where m_V originates through the spontaneous breaking of $U(1)_V$. In the latter case, (1) is extended by, $\mathcal{L}_\phi = |D_\mu \phi|^2 - V(\phi)$ with the dark Higgs field $\phi = 1/\sqrt{2}(v' + h')$ in unitary gauge and after spontaneous symmetry breaking. The $U(1)_V$ covariant derivative is $D_\mu = \partial_\mu + ie'V_\mu$, so that $m_V = e'v'$. The interactions between the physical field h' and V_μ are given by,

$$\mathcal{L}_{\text{int}} = e' m_V h' V_\mu^2 + \frac{1}{2} e'^2 h'^2 V_\mu^2. \quad (2)$$

The crucial difference between the two cases comes in the small m_V limit: while all processes of production or absorption of V in SC are suppressed, $\Gamma_{\text{SC}} \sim O(m_V^2)$, in HC there is no decoupling, and $\Gamma_{\text{HC}} \sim O(m_V^0)$. Indeed, in the limit $m_{V,h'} \rightarrow 0$ the V - h' interaction with external electromagnetic (EM) charge is equivalent to the interaction of charged scalar field quanta with the effective EM charge of $e_{\text{eff}} = \kappa e'$ [1, 7]. Thus, the emission of particles from the $U(1)_V$ sector is generically given by

$$\text{SC} : \gamma^{(*)} \rightarrow V; \quad \text{HC} : \gamma^{(*)} \rightarrow V h', \quad (3)$$

where $\gamma^{(*)}$ is any—virtual or real—photon. The ionization of an atom A in the detector can then be schematically described as

$$\text{SC} : V + A \rightarrow A^+ + e^-, \quad (4)$$

$$\text{HC} : V(h') + A \rightarrow h'(V) + A^+ + e^-, \quad (5)$$

where again all interactions are mediated by $\gamma^{(*)}$.

Solar flux The solar flux of dark photons in the SC is thoroughly calculated in Ref. [6]. In the small mass region, $m_V \ll \omega_p$ where ω_p is the plasma frequency, the emission of longitudinal modes of V dominates the total flux, and the emission power of dark photons per volume can be approximated as

$$\frac{dP_L}{dV} \approx \frac{1}{4\pi} \frac{\kappa^2 m_V^2 \omega_p^3}{e^{\omega_p/T} - 1}. \quad (6)$$

For the purpose of this paper, a more useful quantity is the energy-differential flux of dark photons at the location of the Earth. The spectra for some representative values of the parameters are shown in Fig. 1.

We now turn to the HC: as already mentioned, in the small m_V region, the Higgs-strahlung process dominates the flux, whereas in the region where m_V is comparable to the plasma frequency inside the Sun, $\omega_p = O(100 \text{ eV})$, this process is subdominant due to phase space suppression. In vacuum only an off-shell photon can convert to V . Inside a medium, however, the pole position is shifted and the $\gamma^{(*)} \rightarrow V$ process is equivalent to the decay of either a “massive” transverse mode or a (longitudinal) plasmon. Inside the Sun, since transverse photons are

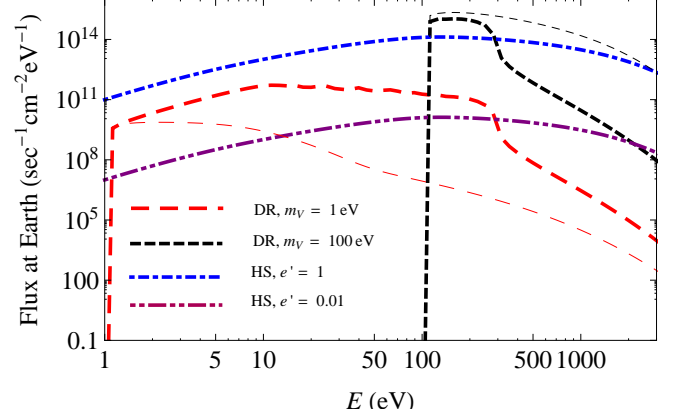


FIG. 1: Fluxes at the Earth as functions of energy for both the SC and HC dark photon for $\kappa = 10^{-12}$. The red and black thick dashed curves show the contribution from longitudinal dark radiation (DR) for $m_V = 1 \text{ eV}$ and 100 eV , respectively. The corresponding thin curves show the transverse contribution. The blue and purple dotted dashed curves show the contribution from the Higgs-strahlung process for $e' = 1$ and 0.01 , respectively.

more numerous than plasmons ($\omega_p^3 \ll T^3$), the Higgs-strahlung process is dominated by the decay of transverse photons. The corresponding matrix element can be written as

$$\mathcal{M} = e' \kappa \varepsilon_\mu^T(q) (k_1 - k_2)^\mu, \quad (7)$$

where k_1 and k_2 are the four-momenta of the outgoing dark Higgs, $q = k_1 + k_2$ is the four-momentum of the decaying photon with transverse polarization vector ε_μ^T , and $q^2 \approx \omega_p^2$. Therefore, the total energy power density of dark radiation contributed by the Higgs-strahlung (HS) process can be estimated as

$$\left. \frac{dP}{dV} \right|_{\text{HS}} \approx \int \frac{d\Phi_2 d^3 \vec{q}}{2q^0 (2\pi)^3} \frac{2\omega}{e^{\frac{q^0}{T}} - 1} |\mathcal{M}|^2 = \frac{e_{\text{eff}}^2 \omega_p^5}{48\pi^3} f\left(\frac{\omega_p}{T}\right), \quad (8)$$

where $d\Phi_2$ is the two-body phase space of the final state, $|\mathcal{M}|^2$ averages over the polarization of the transverse photons, and $f(a) = \int_1^\infty dx (x^2 - 1)^{1/2} x / (e^{ax} - 1)$. From the matrix element (7), we can also calculate the joint differential production rate of the dark vectors and Higgses, which can be written as

$$\left. \frac{d\Gamma^\phi}{dV d\omega} \right|_{\text{HS}} = \frac{e_{\text{eff}}^2 \omega_p^2}{4\pi^3} \int_{\omega + \frac{\omega_p^2}{4\omega}}^\infty \frac{dq^0 (\omega q^0 - \omega^2 - \omega_p^2/4)}{(e^{q^0/T} - 1) [(q^0)^2 - \omega_p^2]}. \quad (9)$$

It is important to note that for small m_V if medium effects restore the $U(1)_V$ symmetry by driving $v' \rightarrow 0$, the Higgs-strahlung rate remains valid. The flux of dark photons on the Earth in the HC for small $m_{V(h')}$ is also shown in Fig. 1. As can be seen, the flux of $V(h')$ is not enhanced in the IR but rather attains a broad maximum at energies $\omega \sim 100 \text{ eV}$.

Absorption of dark photons To calculate the absorption rate of dark photons in the detector's material (4), we need to know the photo-electric absorption cross section σ_{abs} and the index of refraction, encoded in the real and imaginary part of ε_r , the relative permittivity of the target material.

In the SC, the amplitude for the absorption of a dark photon consists of the atomic transition matrix element multiplied by the propagator of $\gamma^{(*)}$. According to Ref. [6], it can be written as

$$\mathcal{M}_{i \rightarrow f+V_{T,L}} = -\frac{\kappa m_V^2}{m_V^2 - \Pi_{T,L}} \langle f | [e J_{\text{em}}^\mu] | i \rangle \epsilon_\mu^{T,L}, \quad (10)$$

where $\epsilon_\mu^{T,L}$ are the polarization vectors for the transverse and longitudinal modes, ($\epsilon_\mu^2 = -1$), and $\Pi_{T,L}$ are defined via the polarization tensor inside the medium of the detector:

$$\Pi^{\mu\nu} \equiv e^2 \langle J_{\text{em}}^\mu, J_{\text{em}}^\nu \rangle = \Pi_T \sum_{i=1,2} \epsilon_i^{T\mu} \epsilon_i^{T\nu} + \Pi_L \epsilon^{L\mu} \epsilon^{L\nu}. \quad (11)$$

The total absorption rate can be written as

$$\Gamma_{T,L}(\omega) = \frac{\kappa_{T,L}^2 e^2 \epsilon_\mu^{T,L*} \epsilon_\nu^{T,L}}{2\omega} \int d^4x e^{iqx} \langle i | J_{\text{em}}^{\mu\dagger}(x) J_{\text{em}}^\nu(0) | i \rangle, \quad (12)$$

where $\kappa_{T,L}$ are the effective mixings for the transverse and longitudinal modes respectively,

$$\kappa_{T,L}^2 = \frac{\kappa^2 m_V^4}{(m_V^2 - \text{Re } \Pi_{T,L})^2 + (\text{Im } \Pi_{T,L})^2}. \quad (13)$$

In (12), the correlation function should be taken in the physical region $\omega > 0$ where it is equal to $-2\text{Im} \langle J_{\text{em}}^{\mu\dagger}, J_{\text{em}}^\nu \rangle = e^{-2}\text{Im} \Pi^{\mu\nu}$ by unitarity (see, e.g. [8]). Therefore, the total absorption rate can be simplified to

$$\Gamma_{T,L} = -\frac{\kappa_{T,L}^2 \text{Im} \Pi_{T,L}}{\omega}. \quad (14)$$

Finally, in an isotropic non-magnetic material one has

$$\Pi_T = -\omega^2 \Delta\varepsilon_r, \quad \Pi_L = -m_V^2 \Delta\varepsilon_r, \quad (15)$$

where $\Delta\varepsilon_r \equiv \varepsilon_r - 1$. Combining Eqs. (13) and (14) we build the main formulae for the absorption rates of the transverse and longitudinal modes:

$$\begin{aligned} \Gamma_T &= \left(\frac{\kappa^2 m_V^4 \text{Im } \varepsilon_r}{\omega^3 |\Delta\varepsilon_r|^2} \right) \left[1 + \frac{2m_V^2 \omega^2 \text{Re } \Delta\varepsilon_r + m_V^4}{\omega^4 |\Delta\varepsilon_r|^2} \right]^{-1}, \\ \Gamma_L &= \frac{\kappa^2 m_V^2 \text{Im } \varepsilon_r}{\omega |\varepsilon_r|^2}. \end{aligned} \quad (16)$$

One can see that in the region $m_V^2 \ll \omega^2 |\Delta\varepsilon_r|$, the absorption rate of the T -modes scales as m_V^4 whereas for the L -mode, it is always proportional to m_V^2 . In the opposite limit, Eq. (16) is given by the number density of

atoms n_A , σ_{abs} , and the velocity of dark photons v_V , $\Gamma_T = \kappa^2 \omega \text{Im } \varepsilon_r = \kappa^2 n_A v_V^{-1} \sigma_{abs}$, (we work in $c = 1$ units).

Going over to the HC, we take $m_{h'} \sim m_V$, and consider the absorption process (5) in the limit of both masses being small. Using the equivalence to the scattering of charged scalars, we write the amplitude as

$$\mathcal{M} = e_{\text{eff}} (k_1 + k_2)^\mu \langle A_\mu, A_\nu \rangle \langle f | J_{\text{em}}^\nu(q) | i \rangle, \quad (17)$$

where k_1 and k_2 are the four momenta of the incoming and outgoing ϕ particles and $q = k_1 - k_2$. Medium-corrected photon propagators $\langle A_\mu, A_\nu \rangle$ in the Coulomb gauge are given by

$$\langle A^i, A^j \rangle = \frac{\delta^{ij} - \hat{q}^i \hat{q}^j}{q^2 - \Pi_T}, \quad \langle A^0, A^0 \rangle = \frac{q^2}{|\vec{q}|^2 (q^2 - \Pi_L)}, \quad (18)$$

where $\hat{q} \equiv \vec{q}/|\vec{q}|$. Following the same steps as in the SC, summing over all the possible excited atomic states in the medium, we get

$$\sum_f |\mathcal{M}|^2 \approx -8e_{\text{eff}}^2 \text{Im } \varepsilon_r \frac{q^2 k_1^0 (k_1^0 - q^0)}{|q^2 + q^0{}^2 \Delta\varepsilon_r|^2}, \quad (19)$$

where terms with further suppression by $\Delta\varepsilon_r$ are omitted. The differential scattering rate with respect to the energy transfer to atoms q^0 is given by,

$$\frac{d\Gamma}{dq^0} \approx \frac{e_{\text{eff}}^2}{4\pi^2} \frac{k_1^0 - q^0}{k_1^0} \left[\log \left(\frac{4k_1^0 (k_1^0 - q^0)}{(q^0)^2 |\Delta\varepsilon_r|} \right) - 1 \right] \text{Im } \varepsilon_r(q^0), \quad (20)$$

Notice that the collinear divergence is regularized by the in-medium modification of the photon propagator.

Limits from direct detection Having obtained both solar fluxes and the absorption rates of dark photons, we are ready to calculate the experimental event rate. In a given experiment, the expected number of signal events in the SC can be written as

$$N_{\text{exp}} = VT \int_{\omega_{\text{min}}}^{\omega_{\text{max}}} \frac{\omega d\omega}{|\vec{q}|} \left(\frac{d\Phi_T}{d\omega} \Gamma_T + \frac{d\Phi_L}{d\omega} \Gamma_L \right) \text{Br}, \quad (21)$$

where V and T are the fiducial volume and live time of the experiment, respectively, and Br is the branching ratio to the desired signal. In general, ε_r depends on both the injecting energy ω and \vec{q}^2 . The latter is suppressed by $\sim \vec{q}^2/(\omega m_e)$ and to good accuracy can be neglected.

Since both $\text{Re } \varepsilon_r$ and $\text{Im } \varepsilon_r$ are proportional to the number density of atoms of the material, n_A , in the small m_V limit $\Gamma_T \propto n_A^{-1}$. As a result, low density materials are best suited for the detection of T -modes. However, as discussed in Ref. [6], the major component of the dark photon flux from the Sun is longitudinal, and from Eq. (16) we have $\Gamma_L \propto n_A$. Therefore, the detection abilities are directly proportional to the total active mass inside the detector. Given the significant enhancement

in the low-energy part of the solar dark photon spectrum, Fig. 1, a detector with a low threshold energy of $O(100)$ eV will have a clear advantage. To date, the only work that considers limits on dark photons from direct DM detection is by HPGe collaboration, Ref. [9]. However, it used incomplete calculations of the solar flux, and as we will show in the following, the low-energy ionization signals by the XENON10 [10] and CoGeNT [11, 12] collaborations yield far more stringent limits.

The XENON10 collaboration has published a study on low-energy ionization events in [10]. With 12.1 eV ionization energy, the absorption of a dark photon with 300 eV energy can produce about 25 electrons. To get a conservative constraint we count all the ionization events within 20 keV nuclear recoil equivalent in Ref. [10], which corresponds to a signal of about 80 electrons. The total number of events is 246, which indicates a 90% C.L. upper limit on the detecting rate to be $r < 19.3$ events $\text{kg}^{-1}\text{day}^{-1}$ (similar to limits deduced in Ref. [13]). In the region $12.1 \text{ eV} < \omega < 300 \text{ eV}$ the ionization process dominates the absorption, and therefore Br in this region can be set to unity. The 90% C.L. upper limit on κ as a function of m_V is shown by the dot-dashed black curve in Fig. 2, where we can see that it gives the most stringent constraint in the SC. To arrive at these limits we reconstruct ε_r for Xe, in the energy domain above the ionization threshold using published data on photoabsorption [14]. The improvement over other experimental probes is quite significant, considering that the signal scales as κ^4 . We also collate main constraints in Table I.

The published data from the CoGeNT DM experiment have a threshold of about 450 eV [12]. In this region, the dark photon flux from the Sun drops almost exponentially with energy, whereas the observed spectrum in CoGeNT is relatively flat. Therefore, in order to optimize the sensitivity, we only use the event counts in the interval 450 – 500 eV and the 90% upper limit on the background subtracted rate is $r < 0.6$ events $\text{kg}^{-1}\text{day}^{-1}$. The resulting sensitivity is shown as the thick dotted purple curve in Fig. 2, which is far weaker than the constraint from the energy loss of the Sun. Hence CoGeNT does not have sensitivity to constrain dark photons since the required flux is not supported by the Sun.

In the HC, N_{exp} in Eq. (21) must include a contribution from (20), and it dominates in the region $m_V^2 \ll \omega^2 |\Delta\varepsilon_r|$, but is subdominant if $m_V^2 \sim \omega^2 |\Delta\varepsilon_r|$. Since the flux of $V(h')$ in the HC is mainly contributed from conversion of transverse photons in the Sun, the spectral distribution reflects the solar temperature, Fig. 1, with the cutoff above 1 keV. A dark photon of 1 keV energy can at most produce about 60 electrons in liquid xenon. For $e' = 0.1$, the 90% C.L. upper limit is shown as the thin dot-dashed curve in Fig. 2. For the sensitivity from CoGeNT we take into account all the events from 450 eV to 1 keV and the associated constraint is shown as the thin dotted curve

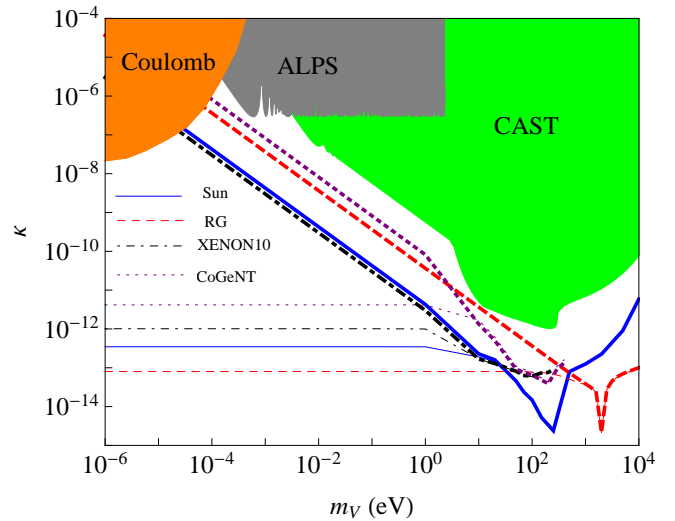


FIG. 2: Constraints on κ as functions of m_V . The solid, dashed, dot-dashed and dotted curves show constraints from the energy loss of the Sun by requiring that the dark photon luminosity does not exceed 10% of the standard solar luminosity [15], energy loss of red giant stars (RG), the XENON10 experiment and the CoGeNT experiment, respectively. The thick curves are for the SC, whereas the thin curves are for the HC with $e' = 0.1$. For comparison, the current bound (gray shading) from the LSW-type experiments are shown (see Ref. [16] for details). The conservative constraint from the CAST experiment [17] by considering the contributions from only the transverse modes [4] is also shown in green shading. The orange shaded region is excluded from tests of the inverse square law of the Coulomb interaction [18].

TABLE I: Sensitivities to κ and e_{eff} in the small m_V region.

Model param.	Sun	RG	XENON10	CoGeNT
SC, $\kappa \times \frac{m_V}{\text{eV}}$	4×10^{-12}	4×10^{-11}	3×10^{-12}	8×10^{-11}
HC, e_{eff}	3×10^{-14}	8×10^{-15}	1×10^{-13}	4×10^{-13}

in Fig. 2, and included in Table I as limit on e_{eff} .

Conclusions We point out that the unprecedented sensitivity of some of the DM experiments to ionization allows to turn them into the most sensitive dark photon helioscopes. By directly calculating the ionization signal, we show that the ensuing constraint from the XENON10 experiment significantly surpasses any other bounds on dark photons, including very tight stellar energy loss constraints in the m_V -interval from 10^{-5} to 100 eV. In the case of “mini-charged” particles (equivalent to the Higgsed version of dark photons), we also derive a stringent bound, $e_{\text{eff}} < 10^{-13}$, which is second only to the red giant energy loss constraint; see also [19]. Given the enormous amount of experimental progress in the field of direct DM detection, one can be optimistic that future sensitivity to dark photons, and other light particles is bound to be further improved.

Acknowledgements We acknowledge useful correspondence with G. Raffelt and J. Redondo on stellar production rates and the strength of the solar luminosity constraint. Research at the Perimeter Institute is supported in part by the Government of Canada through NSERC and by the Province of Ontario through MEDT.

-
- [1] B. Holdom, Phys. Lett. B **166**, 196 (1986). L. B. Okun, Sov. Phys. JETP **56**, 502 (1982) [Zh. Eksp. Teor. Fiz. **83**, 892 (1982)].
 - [2] J. Jaeckel and A. Ringwald, Ann. Rev. Nucl. Part. Sci. **60**, 405 (2010) [arXiv:1002.0329 [hep-ph]].
 - [3] M. Ahlers, H. Gies, J. Jaeckel, J. Redondo and A. Ringwald, Phys. Rev. D **77**, 095001 (2008) [arXiv:0711.4991 [hep-ph]].
 - [4] J. Redondo, JCAP **0807**, 008 (2008) [arXiv:0801.1527 [hep-ph]].
 - [5] G. G. Raffelt, The astrophysics of neutrinos, axions, and other weakly interacting particles,” Chicago, USA: Univ. Pr. (1996) 664 p
 - [6] H. An, M. Pospelov and J. Pradler, arXiv:1302.3884 [hep-ph].
 - [7] S. Davidson, B. Campbell and D. C. Bailey, Phys. Rev. D **43**, 2314 (1991); S. Davidson, S. Hannestad and G. Raffelt, JHEP **0005**, 003 (2000) [hep-ph/0001179].
 - [8] C. Itzykson and J.-B. Zuber, *Quantum Field Theory*, (McGraw-Hill Book Company, New York, 1980).
 - [9] R. Horvat, D. Kekez, M. Krcmar, Z. Krecak and A. Ljubicic, arXiv:1210.1043 [hep-ex].
 - [10] J. Angle *et al.* [XENON10 Collaboration], Phys. Rev. Lett. **107**, 051301 (2011) [arXiv:1104.3088 [astro-ph.CO]].
 - [11] C. E. Aalseth, P. S. Barbeau, J. Colaresi, J. I. Collar, J. Diaz Leon, J. E. Fast, N. Fields and T. W. Hossbach *et al.*, Phys. Rev. Lett. **107**, 141301 (2011) [arXiv:1106.0650 [astro-ph.CO]].
 - [12] C. E. Aalseth *et al.* [CoGeNT Collaboration], arXiv:1208.5737 [astro-ph.CO].
 - [13] R. Essig, A. Manalaysay, J. Mardon, P. Sorensen and T. Volansky, Phys. Rev. Lett. **109**, 021301 (2012) [arXiv:1206.2644 [astro-ph.CO]].
 - [14] B.L. Henke, E.M. Gullikson, J.C. Davis, Atomic Data and Nuclear Data Tables 54, 181-342, (1993).
 - [15] P. Gondolo and G. Raffelt, Phys. Rev. D **79**, 107301 (2009) [arXiv:0807.2926 [astro-ph]].
 - [16] K. Ehret, M. Frede, S. Ghazaryan, M. Hildebrandt, E. - A. Knabbe, D. Kracht, A. Lindner and J. List *et al.*, Phys. Lett. B **689**, 149 (2010) [arXiv:1004.1313 [hep-ex]].
 - [17] S. Andriamonje *et al.* [CAST Collaboration], JCAP **0704**, 010 (2007) [hep-ex/0702006].
 - [18] D. F. Bartlett and S. Loegl, Phys. Rev. Lett. **61**, 2285 (1988).
 - [19] M. Ahlers, J. Jaeckel, J. Redondo and A. Ringwald, Phys. Rev. D **78**, 075005 (2008) [arXiv:0807.4143 [hep-ph]].